

Parabolic heater for low crosstalk digital optical switch

ABU SAHMAH M. SUPA'AT, SEVIA M. IDRUS,

A. B. MOHAMMAD, IAN YULIANTI*, ABDULAZIZ M. AL-HETAR

Photonics Technology Centre, Faculty of Electrical Engineering, Universiti Teknologi Malaysia, 81310 Johor, Malaysia

A new design method is proposed to optimize a heater shape in Digital Optical Switch (DOS) in order to improve the crosstalk performance. The heater has been optimized so that the thermal field distribution induce a constant effective refractive index difference (ΔN_{eff}) along the propagation direction. Compare to the linear heater, the result shows that the DOS using parabolic heater could improve the crosstalk performance. At temperature change of 30 °C, the crosstalk achieved by linear heater is only -10.3 dB, while the crosstalk achieved by the parabolic heater is -22.5 dB.

(Received May 6, 2009; accepted May 25, 2009)

Keyword: Digital optical switch, Heater, crosstalk, Temperature distribution

1. Introduction

Having the advantages of simplicity and flexibility, thermo optic effect has been widely applied in optical switch to accomplish light provisioning. Thermo-optic effect allows the change of refractive index by introducing temperature change to waveguide materials. For materials having negative thermo-optic coefficient (TOC) such as polymers, the refractive index decrease as the temperature increase. Meanwhile, for materials with positive TOC such as silica, the refractive index increase as the temperature increase.

The thermo-optic switches are divided into three basic types: digital optical switches (DOS) interferometric switches and directional coupler (DC). Interferometric switches are usually made in silica or polymer in Mach-Zehnder and directional coupler arrangement [1]. Despite its low power consumption, MZI has some drawbacks such as polarization and wavelength sensitive. The advantage of the DOS over the MZI and DC switch is its sensitivity for drive power fluctuations, polarization, wavelength, and temperature and device geometrical variations [2].

The operation of the DOS is based on the modal effective index variation induced by waveguide heating, which can modify the beam propagation pattern inside the structure. A signal launched in the input channel will adiabatically evolve to the local fundamental mode of the waveguide having the highest effective refractive index. The output channel will be the channel with the highest effective refractive index. The waveguide heating may be accomplished by applying current to the heater electrode located at selected sections of the structure.

In most of the DOS available today, the heater is designed to be linear in shape and is located directly on top of the waveguide. By locating the heater in this way, the heater will be in very close proximity to the other branch [3]. Hence, some undesirable degree of heating will occur in the branch which is not intended to be heated.

As the effect, the efficiency of the switch will decreased because a large part of the input field will be guided into the unheated waveguide causing the higher crosstalk (CT) at the end of the switch. Moreover, the effective refractive index difference between branches (ΔN_{eff}) induced by this type of heater is not constant along the propagation direction. This condition does not agree with the most of Y-junction structure optimization methods which usually assume the constant ΔN_{eff} along the propagation direction, such as in the coupled mode theory (CMT) [4-6] and beam propagation method (BPM) [7,8].

In this paper, a new design of heater to be used in DOS is proposed. The light propagation in the switch has been simulated using finite difference beam propagation method (FD-BPM) by introducing a constant refractive index difference between waveguides. The heater lateral position has been optimized so that the thermal distribution induces a constant ΔN_{eff} . To determined the ΔN_{eff} induced by the heater, the thermal distribution and the modal analysis has been analyzed using finite difference method (FDM) accomplished by MATLAB. For validation purpose, a three-dimensional beam propagation that includes the effects of heater has also been performed using FD-BPM.

2. Heater optimization

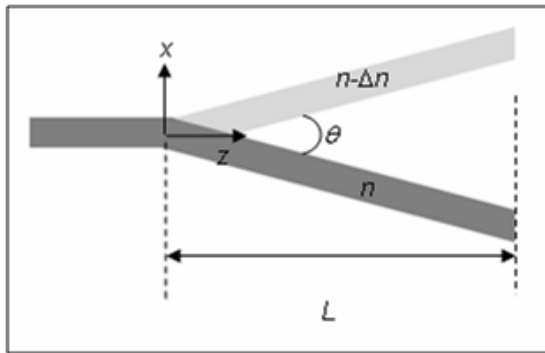
The heater has been designed so that the ΔN_{eff} induced by the heater is constant along the propagation constant. This consideration was taken in order to satisfy the initial condition in the BPM and other methods such as CMT that assume the constant ΔN_{eff} along the propagation distance in the optimization of the Y-junction structure.

The optimum position of the heater is dependent on the geometry (layer thicknesses, height, and width of the waveguide) and the material properties (thermal conductivity, refractive index, thermo-optic coefficient), hence it will be different for each type of switch. In this

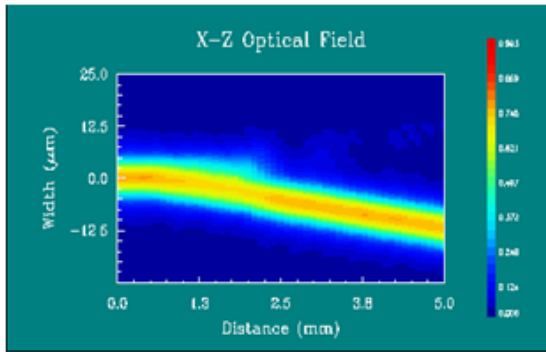
work, the heater optimization was done for linear Y-junction in which the dimension and specifications are presented in section 2.1. The crosstalk performance obtained from simulation by introducing constant refractive index difference manually is also presented in section 2.1. However, the method presented here is applicable for any Y-junction shape.

2.1 Y-junction structure

The waveguide used in this simulation is buried square core waveguide (BSC) with a core size of $7 \times 7 \mu\text{m}^2$. The core-cladding refractive index difference has been optimized so that the waveguide operate as single-mode waveguide in the optical communication transmission window. The core and cladding refractive index are determined to be 1.464 and 1.459, respectively [9, 10]. The thickness of upper cladding and the lower cladding were determined $10 \mu\text{m}$ and $20 \mu\text{m}$ respectively, to avoid the attenuation to the heater and to the substrate.



a



b

Fig.1. (a) Y-junction geometry with constant refractive index difference between branches, (b) light propagation in the Y-junction at Δn of 0.002 ($\Delta N_{eff} = 0.00127689$).

The branching angle (θ) and the length (L) of the Y-junction structure were determined to be 0.299° and 4.55 mm, respectively. The branching angle was chosen to be relatively large in order to make the fabrication process less difficult. The performance of the Y-junction structure

was analyzed by introducing a constant small refractive index difference (Δn) along propagation distance. The refractive index difference was introduced manually by directly changing the refractive index value of one of the Y-junction arms in the simulation. In this step, the thermo-optic effect induced by a heater was not applied. By changing the refractive index of one of the arms, the light is guided to the branch with the higher refractive index and thus the crosstalk performance of the Y-junction structure as function of refractive index difference could be obtained. The simulation has been done for TE mode at $1.55 \mu\text{m}$ of wavelength while the Δn was varied from 0.0002 up to 0.003. The Y-junction geometry and the light propagation in the Y-junction are depicted in Fig.1.

The effective refractive index (N_{eff}) of the branch for each refractive index value was determined by using finite difference-alternating direction implicit (ADI) mode solver 3D. The CT response to ΔN_{eff} was plotted in Fig.2.

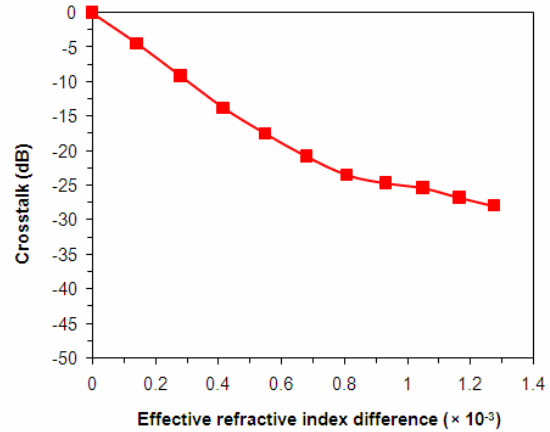


Fig. 2. Crosstalk as function of effective refractive index difference between branches of the Y-junction.

The simulation result shows that the crosstalk of -25 dB could be achieved by introducing ΔN_{eff} of 0.001.

2.2 Thermal analysis

Thermal analysis is an important step to be carried out in designing heater electrode accomplishing switching function in the DOS. The main aim of thermal analysis is to determine the temperature profiles in the waveguide induced by the heater. To evaluate the thermal transient of the switch, the equation to be solved is the heat transfer equation in transient condition with constant thermal conductivity:

$$k\nabla^2 T + Q(x, y, z, t) = \rho c_p \frac{\partial T}{\partial t} \quad (1)$$

where ρ is the material density, c_p is the specific heat, k is the thermal conductivity and $Q(x,y,z,t)$ is the heat generation rate per unit volume.

For steady state heat conduction, Eq. (1) can be deduced to

$$k\nabla^2 T + Q(x, y, z, t) = 0 \quad (2)$$

The thermal distribution in the waveguide was analyzed by considering both convection and conduction mechanism as proposed by Ibrahim *et al.* [11].

Since the length of the heater is much longer than the width of the heater, the two dimensional analysis is used [12]. Therefore, the governing equation for steady-state heat conduction is then defined by:

$$k\left(\frac{\partial^2 T(x, y)}{\partial x^2} + \frac{\partial^2 T(x, y)}{\partial y^2}\right) + Q(x, y, z, t) = 0 \quad (3)$$

The thermal conductivity of core and cladding material are assumed to be identical. In this work, the material used is polymer with thermal conductivity of $0.2 \text{ Wm}^{-1}\text{C}^{-1}$.

In order to determine the temperature distribution, the appropriate forms of the steady-state heat conduction equation need to be defined using the boundary condition. The boundary condition for this simulation is illustrated in Fig. 3.

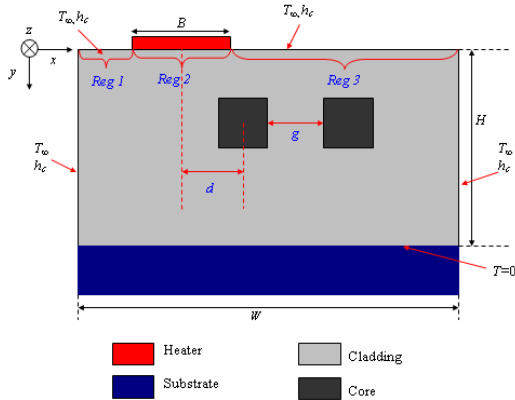


Fig.3. Boundary condition illustration of Y-junction cross section with a heater electrode at certain point in the z-direction.

The left side and the right side of the waveguide are subjected to the convection, thus the boundary condition applied in this side is a *convective surface condition* where the convection rate equation is defined by

- for left side surface:

$$-k \frac{\partial T}{\partial x} \Big|_{x=0} = h_c (T|_{x=0} - T_\infty) \quad (4)$$

- for right side surface:

$$-k \frac{\partial T}{\partial x} \Big|_{x=W} = h_c (T|_{x=W} - T_\infty) \quad (5)$$

where h_c is the heat transfer coefficient of air and T_∞ is the air upstream temperature which is assumed to be 25°C .

At the top surface, the boundary condition is specified in three regions (Fig.3):

- *Region 1 and region 3*

The surface is subjected to the convection.

$$-k \frac{\partial T}{\partial x} \Big|_{y=0} = h_c (T|_{y=0} - T_\infty) \quad (6)$$

- *Region 2*

The surface is subjected to the heat flux originated from the heater electrode. The boundary condition applied in this region is the *Newman boundary condition* with the constant heat flux.

$$-k \frac{\partial T}{\partial y} \Big|_{y=0} = \frac{P}{BL_h} \quad (7)$$

where P is the applied power, B is the heater width and L_h is the heater length.

At the bottom surface, the silicon substrate is considered as a perfect heat sink due to its high thermal conductivity. The temperature assumed to be [13]

$$T|_{y=H} = 0 \quad (8)$$

The equations derived above are solved by using numerical method. The numerical method applied in this work is FDM by employing successive over relaxation (SOR) as an iterative method in order to enhance the rate of convergence [14].

2.3 Heater lateral position optimization

The temperature distribution obtained from finite difference method is used to determine the spatial perturbation of the refractive index in the structure through the TOC, dn/dT of the material. For polymer material used, the TOC value is $-1.7 \times 10^{-4} \text{C}^{-1}$. This perturbation is then incorporated into scalar *Helmholtz* wave equation of TE mode as defined by:

$$\frac{\partial^2 E}{\partial x^2} + \frac{\partial^2 E}{\partial y^2} + (k_o^2 n^2 - \beta^2)E = 0 \quad (9)$$

where k_o is the wave number; x , y and z are the coordinates corresponding to the lateral, transverse and propagation directions, respectively. This scalar *Helmholtz* wave equation is solved for fundamental mode by using FDM to determine the new effective refractive index for each branch. The propagation constants (β) of the branches are calculated by considering that the branches are perfectly separated such that there is no coupling between channel modes [15, 16]. In this work, the source code for thermal FDM has been integrated with the modal analysis FDM so that the ΔN_{eff} induced by the heater can be directly determined.

The heater lateral position is optimized by determining the ΔN_{eff} (for a constant width) for various heater lateral positions, d as shown in Fig.3. This procedure is repeated for a number of cross-sections varying from the branching point until the end of the Y-junction. This is done by varying the waveguide gap, g as shown in Fig.3. The optimal heater lateral positions as function of z (propagation direction) are determined to be the lateral position which exhibit the same value for ΔN_{eff} in all cross-sections.

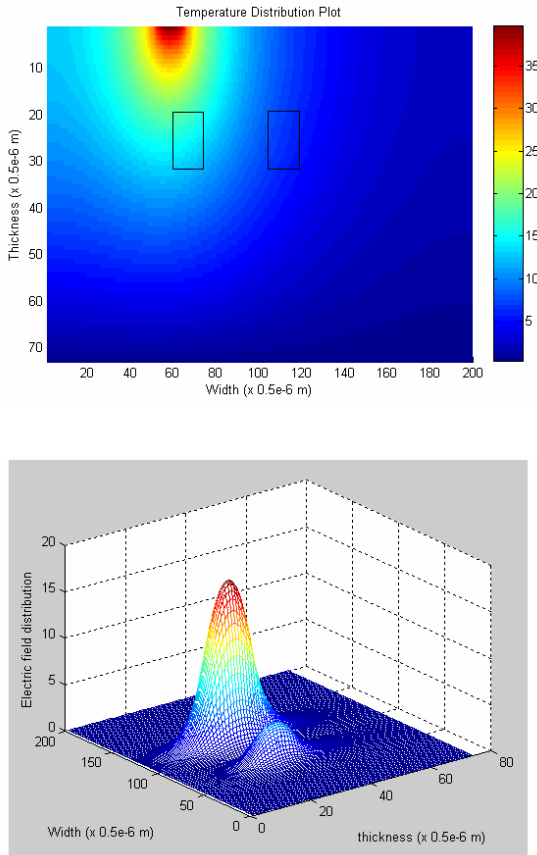


Fig.4. (a) The temperature distribution induced by the heater with applied power of 37.5 mW, $g = 16 \mu\text{m}$ and $d=0$ (b) Electric field distribution due to the induced temperature by considering that there is no coupling between branches.

For the sake of simplicity, the heater width (B) was chosen to be the same as the core width which is $7 \mu\text{m}$ [17]. The heater length was chosen to be the same as the Y-junction length as a trade off between the crosstalk value and the power consumption. To optimize the increased temperature at the core when $d=0$, the power applied was determined to be 37.5 mW. The thermal field distribution induced by the heater located directly at the top of the waveguide ($d=0$) with applied power of 37.5 mW at the end of the branches is depicted in Fig.4 (a). The maximum temperature at the heater and the cladding top surface interface is around 48°C and the increased temperature at the core is around 20°C .

The electric field distribution in the heated branch and the unheated branch induced by the refractive index perturbation due to the temperature change is also depicted in Fig.4 (b). The effective refractive index obtained from the simulation for the heated branch and for the unheated branch are 1.4582795 and 1.4595592, respectively. The ΔN_{eff} value of 0.0012797 is achieved for this condition. The ΔN_{eff} as function of d for various waveguide gaps (g) is depicted in Fig.5. It is shown that, for all waveguide gap values, the maximum value of ΔN_{eff} is achieved at d of $8 \mu\text{m}$.

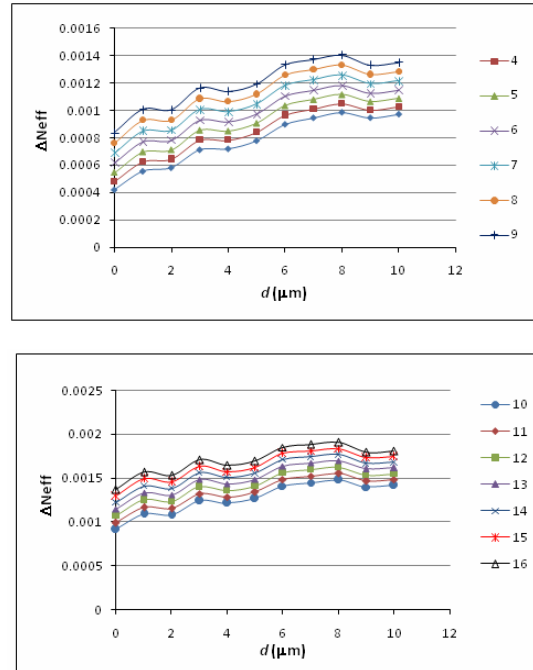


Fig. 5. ΔN_{eff} as function of d for various waveguide gaps.

The graph of ΔN_{eff} as function of d in Fig.5 above are fitted using sixth order polynomial and the equation is used to determine the heater lateral position that induce certain value of ΔN_{eff} .

The heater lateral position as function of propagation distance is depicted in Fig.6. In order to get a smooth

curve of a heater position, the graph is fitted by a second order polynomial as defined by:

$$x(z) = -1 \times 10^{-6} z^2 + 0.005z + 8.9525 \text{ (\mu m)} \quad (10)$$

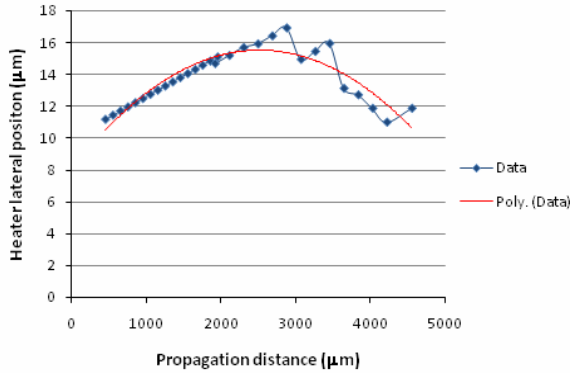


Fig.6. The heater lateral position as function of propagation distance.

Since the second order polynomial equation is the parabolic equation, the heater formed by Eq. (10) is called as parabolic heater. The lay out of a heater using this equation is depicted in Fig.7.

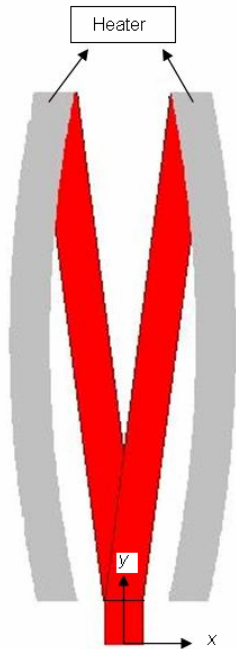


Fig.7. The Y-junction with parabolic heater lay out.

For validation purpose, the effect of the thermal field induced by the parabolic heater to the light propagation in the Y-junction is simulated using BeamProp™. The result

is depicted in Fig.8. As comparison, the crosstalk resulted from constant ΔN_{eff} in Fig.2 is also presented in Fig.8 after converting the ΔN_{eff} in to the temperature change required. The temperature change required to exhibit the ΔN_{eff} value in Fig.2 can be easily obtained from the thermal FDM integrated with the modal analysis FDM which has previously been developed. It is shown that the crosstalk resulted from the refractive index perturbation induced by the parabolic heater almost the same as the simulated crosstalk obtained by changing the constant ΔN_{eff} manually. Slight deviation in the result can be explained as an effect of the difference in numerical methods used by both methods and due to the heater lateral position that not perfectly induce a constant ΔN_{eff} because of the curve fitting. It also can be seen that further increase of temperature change above 30°C may result in crosstalk degradation.

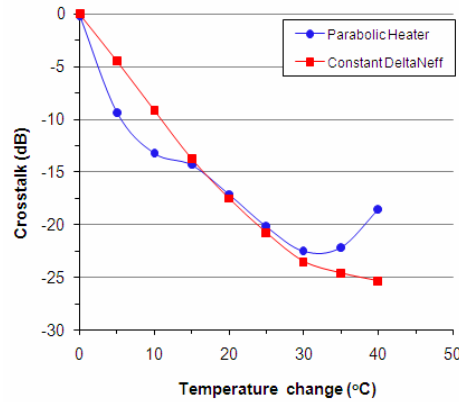


Fig. 8. Simulated crosstalk performance of the Y-junction structure by changing the ΔN_{eff} manually compare to that resulted from temperature change induced by parabolic heater.

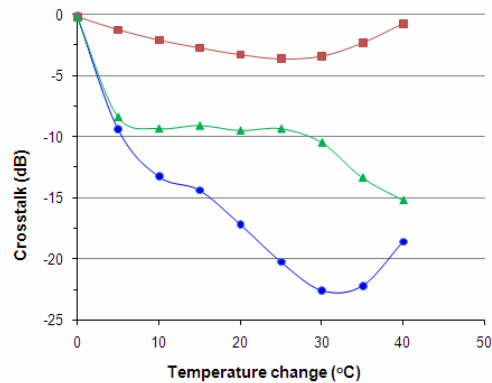


Fig. 9. Comparison of crosstalk performance of parabolic heater and linear heater

As comparison, the simulation was also done for a linear heater, which is located directly on top of the branches and which is shifted by 8 μm from the core center. An offset of 8 μm was chosen since it provide the maximum ΔN_{eff} as shown in Fig. 5. The simulation results show that the parabolic heater better performs the switch function than the linear heater.

By using a linear heater, the light is hardly switched to the unheated branch. For the linear heater, which is located on top of the cores, the crosstalk could not reach -5 dB, even for large temperature change. The crosstalk performance is improved by locating the heater at an offset from the core. However, the crosstalk achieved is still high. Meanwhile, the temperature change induced by the proposed heater could switch the light to the unheated branch efficiently.

The comparison of crosstalk performance of the proposed heater and linear heater is depicted in Fig.9. The crosstalk could be reduced up to -22.5 dB at temperature change of 30°C. Meanwhile, at the same temperature change, the crosstalk achieved by the shifted linear heater is only -10.3 dB.

3. Conclusions

The heater designed using the proposed method in this paper could efficiently improve the switching function. At temperature change of 30°C, the crosstalk achieved by the parabolic heater is -22.5 dB, while the crosstalk achieved by linear heater located on top of the core and shifted by 8 μm from the core are only -3.4 dB and -10.3 dB, respectively. Furthermore, the parabolic heater could satisfy the initial assumption of constant refractive index difference that is usually taken in designing the Y-junction structure for DOS application.

Acknowledgements

The authors would like to thank the Ministry of Science, Technology and Innovation (MOSTI) for funding this research via project no. 01-01-06-sf0162. Our gratitude also goes to the members of Photonics Technology Center (PTC) of Universiti Teknologi Malaysia for their helpful discussions throughout the completion of this work.

References

- [1] A. S. M. Supa'at, M. H. Ibrahim, A. B. Mohammad, N. M. Kassim, N. E. Ghazali, *American Journal of Applied Sciences*. 5 (2008).
- [2] M. B. J. Diemeer, *Optical Materials*. 9 (1998).
- [3] L. Eldada, 2007. U.S. Patent 7302141B2.
- [4] W. K. Burns, *IEEE Photonics Technology Letters*. 4, 861 (1992).
- [5] W. K. Burns, MHowerton, R.P. Moeller, *Journal of Lightwave Technology*. 10 (1992).
- [6] H. Okayama, M. Kawahara, *Journal of Lightwave Technology*. 11, 379 (1993).
- [7] R. Moosburger, C. Kostrzewa, G. Fischbeck, and K. Petermann, *IEEE Photonics Technology Letters*. 9 (1997).
- [8] R. Hauffe, *Integrated Optical Switching Matrices Constructed from Digital Optical Switches Based on Polymeric Rib Waveguides*. PhD Dissertation, Technischen Universitat Berlin. 2002.
- [9] A.S.M. Supa'at, A.B. Mohammad, N.M. Kassim. *Jurnal Teknologi Universiti Teknologi Malaysia*. 40D (2004).
- [10] I. Yulianti, A.S.M. Supa'at, S. M. Idrus, A.B. Mohammad. *Proc.Communication Systems and Networks (AsiaCSN 2008)*, Langkawi, Malaysia, April (2008).
- [11] M. H. Ibrahim, N. M. Kassim, A. B. Mohammad, N. Kamsah. *Jurnal Teknologi Universiti Teknologi Malaysia*. (2007).
- [12] A. S. M. Supaat. *Design and Fabrication of a Polymer Based Directional Coupler Thermo-optic Switch*. Universiti Teknologi Malaysia: PhD Thesis. 2004.
- [13] W.-K. Wang, H. J. Lee, and P. J. Anthony. *IEEE Journal of Lightwave Technology*. 14(1996).
- [14] P. Majumdar. *Computational Methods for Heat and Mass Transfer*. Taylor & Francis Group. New York. 2005.
- [15] W.K. Burns, F. Milton, *IEEE Journal of Quantum Electronics*. QE-11(1975).
- [16] W.K. Burns and F. Milton, *IEEE Journal of Quantum Electronics*. QE-16 (1980).
- [17] X. Jiang, Wei. Qi, H. Zhang, Y. Tang, Y. Hao, J. Yang, M. Wang, *IEEE Photonics Technology Letters*, 18(2006).

*Corresponding author: ianyulianti@yahoo.com